Full Paper

Synthesis, Cytotoxicity, Docking Study, and Tubulin Polymerization Inhibitory Activity of Novel 1-(3,4-Dimethoxyphenyl)-5-(3,4,5-trimethoxyphenyl)-1*H*-1,2,4-triazole-3-carboxanilides

Omar M. Aly[1], Eman A. Beshr[1], Raed M. Maklad[1], Muhamad Mustafa[1], and Amira M. Gamal-Eldeen[2]

[1] Faculty of Pharmacy, Medicinal Chemistry Department, Minia University, Minia, Egypt
[2] Cancer Biology Laboratory, Center of Excellence for Advanced Sciences, National Research Center, Cairo, Egypt

A series of novel 1-(3,4-methoxyphenyl)-5-(3,4,5-trimethoxyphenyl)-1*H*-1,2,4-triazole-3-carboxylic acid derivatives (**4a**–**n**) were synthesized and evaluated for their *in vitro* cytotoxic activity against the growth of four different human cell lines (hepatocarcinoma HepG2, breast adenocarcinoma MCF-7, colon carcinoma DLD-1, and leukemia HL-60). The anilides of *m*-anisidine **4e**, *o*-anisidine **4f**, and 3,5-difluoroaniline **4l** demonstrated best results on MCF-7 cells and mean IC_{50} values of 7.79, 10.79, and 13.20 μM, respectively. The compounds produced a significant reduction in cellular microtubules at a concentration of 25 μg/mL, for microtubule loss. Molecular modeling studies involving compounds **4d**, **4e**, **4f**, and **4l** with the colchicine binding site of α,β-tubulin revealed hydrogen bonding and hydrophobic interactions with several amino acids in the colchicine binding site of β-tubulin.

Keywords: Cytotoxicity / Docking study / 1,2,4-Triazole / Tubulin

Received: March 10, 2014; Revised: March 29, 2014; Accepted: May 5, 2014

DOI 10.1002/ardp.201400096

Introduction

Tubulin polymerization inhibition is the subject of both research and clinical trials, specially those tubulin polymerization inhibitors that have the ability of vascular disrupting activity. Tubulin is the building block of microtubules, which are important in cellular functions such as cell transport, movement, separation of chromosomes during mitosis in addition to the cytoskeleton structure. Anti-microtubule agents are anti-tumor agents that can be categorized into three classes: (i) microtubule-stabilizing agents, (ii) vinca site binding agents, and (iii) colchicine site binding agents. Of the three classes of anti-microtubule agents, colchicine site agents are the only class of agents that do not have a representative drug in clinical use for cancer. However, these agents are structurally the most diverse group among the three classes of tubulin binding agents. They include natural products as well as synthetic small molecules (Fig. 1) [1, 2]. Among all the colchicine site agents, combretastatin A-4 (CA-4) has received special attention in the last few years [3, 4]. In addition to its potent cytotoxicity and inhibitory activity on tubulin polymerization, CA-4 is one of the few anti-microtubule agents reported to have selective vascular disrupting activity [5, 6]. CA-4 and its water-soluble prodrug, combretastatin A-4 phosphate (CA-4P), are selectively cytotoxic to rapidly proliferating tumor vasculature than normal blood vessels, resulting in reduced blood flow to tumor and eventual hemorrhagic necrosis [7, 8]. The anti-tumor and anti-vascular activities of CA-4 analogs have been demonstrated in both animal and human studies [9–12]. Many analogs of CA-4 have been designed to study the structure–activity relationship of the molecule in order to enhance both the cytotoxic and selective vascular disrupting activities [13–24].

Promoted with the above-mentioned studies and as a continuation of our research interest in the synthesis and biological activities of novel tubulin polymerization inhibitors [25, 26], the present study is concerned with the

Correspondence: Dr. Omar M. Aly, Faculty of Pharmacy, Medicinal Chemistry Department, Minia University, Minia 61519, Egypt.
E-mail: omarsokkar@mu.edu.eg
Fax: +20 86 2369075

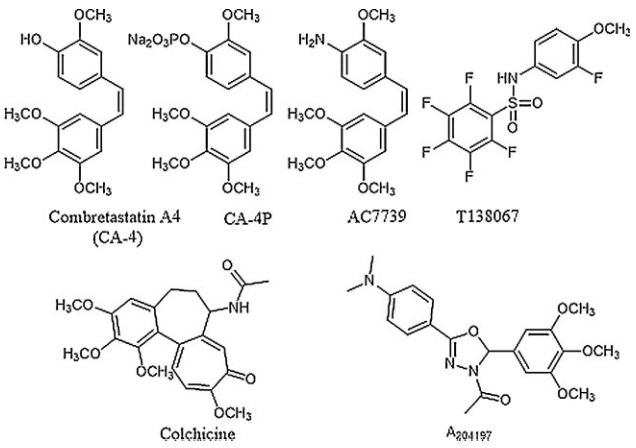

Figure 1. Examples of colchicine and combretastatin analogs.

synthesis of novel 1-(3,4-dimethoxyphenyl)-5-(3,4,5-trimethoxyphenyl)-1*H*-1,2,4-triazole-3-carboxylic acid derivatives with the objective of discovering novel and potent anti-tubulin agents and as a starting point of a full structure–activity relationship study of 1,5-diaryl-1*H*-1,2,4-triazole-3-carboxylic acid derivatives. The ability of the prepared compounds was evaluated for both *in vitro* cytotoxic properties on four different cancer cell lines and tubulin polymerization inhibitory activity. Furthermore, molecular modeling studies of the most active tubulin inhibitor with the colchicine binding site of α,β-tubulin were also performed.

Results and discussion

Chemistry

The synthetic route used to synthesize 1-(3,4-dimethoxyphenyl)-5-(3,4,5-trimethoxyphenyl)-1*H*-1,2,4-triazole-3-carboxanilides **4a–n** is outlined in Scheme 1. Key starting compound, 2-(3,4,5-trimethoxybenzamido)acetic acid **1**, was prepared in good yield (85%) by the reaction of glycine with 3,4,5-trimethoxybenzoyl chloride in 10% NaOH. Heating of compound **1** with acetic anhydride afforded the corresponding compound **2**. The synthesis of the key intermediate **3** was carried out using Kuskov like reaction through coupling of

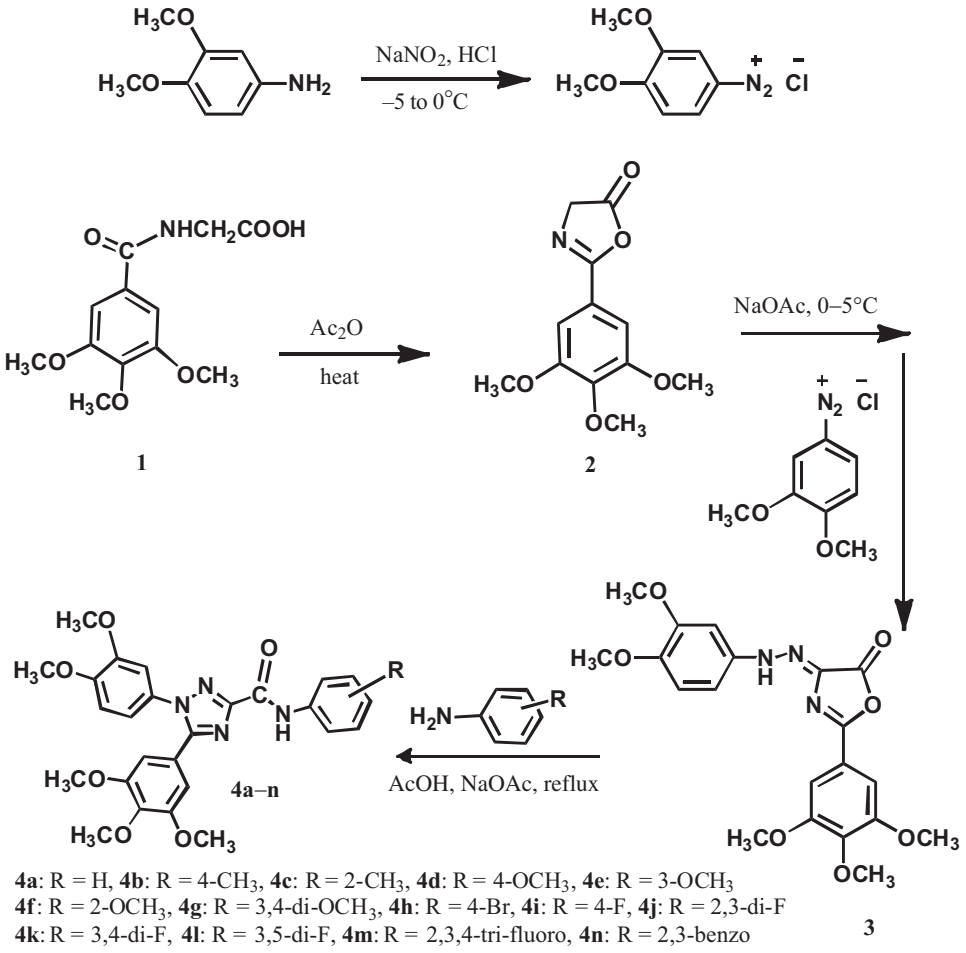

Scheme 1. Synthesis of the target compounds **4a–n**.

the diazonium salt of 3,4-dimethoxyaniline with the active methylene of **2** in presence of sodium acetate. The IR spectrum of **3** revealed the presence of strong stretching band at 1780 cm^{-1} of the C=O group of the lactone ring.

According to Sawdey rearrangement [27, 28], 4-(2-(3,4-dimethoxyphenyl)hydrazono)-2-(3,4,5-trimethoxyphenyl)oxazol-5(4*H*)-one **3** by a variety of nucleophiles opened the oxazoline ring to form acyclic intermediates, which then recyclized via loss of water affording triazole derivatives. Reaction of **3** with primary aromatic amines in mild acidic medium formed the target anilides **4a**–**n** in 53.01–70.20% yield. The physical and spectral data are listed in the Experimental section.

Biological investigations

Anti-tumor activity against four different human cancer cell lines

Using MTT assay, the effect of the tested compounds on the viability of different human cancer cell lines were studied after 48 h of incubation. The treatment of hepatocellular carcinoma HepG2 cells, leukemia HL-60 cells, colon cancer DLD-1 cells, and breast cancer MCF-7 cells with gradual concentrations of different compounds revealed that compounds **4e** and **4f** possessed the highest promising cytotoxic effect against HepG2 cells, compounds **4e**, **4f**, and **4l** demonstrated cytotoxic effect against HL-60 cells, and the tested compounds showed weak cytotoxic effect on DLD-1 cells. Test compounds **4e**, **4f**, **4g**, **4k**, **4l**, and **4m** possessed the highest promising cytotoxic effect on MCF-7 cells as concluded from their IC_{50} values, as shown in Table 1. Anilides of the *para*-substituted anilines like **4b**, **4d**, **4h**, and **4i**, which are anilides of *p*-toluidine, *p*-anisidine, *p*-bromoaniline, and 4-fluoroaniline, respectively, showed decreased activity in comparison with the unsubstituted anilide of aniline **4a** or that of 1-naphthyl amine **4n**. In conclusion, from all anti-tumor experiments, it is clear that anilides with *m*-anisidine **4e** and *o*-anisidine **4f** are multipotential antitumor compounds, since both of them possessed high cytotoxic effect against liver cancer cells HepG2, breast cancer MCF-7 cells, and leukemia HL-60 cells. The highest promising cytotoxic compound is **4e**, which had IC_{50} values of 15.43, 7.97, and 12.97 μM against HepG2, MCF-7 and HL-60 cells, respectively, compared with values of 0.014–0.403 μM for 3-amino-deoxyCA-4 [29].

*Effect of compounds **4a–n** on tubulin polymerization*

The effect of the synthesized compounds on tubulin polymerization was done to investigate whether the cytotoxicity is related to the interaction with tubulin or not. Tubulin was evaluated in MCF-7 cell line after treating with 25 μg/mL of each compound for 48 h using indirect ELISA. The treatment of breast carcinoma MCF-7 cells revealed that compounds **4a**, **4e**, **4f**, **4g**, **4i**, **4k**, **4l**, and **4m** showed a promising inhibitory effect of cellular tubulin, as concluded from their percentage of inhibition (around 50%), as shown in Fig. 2, while the other tested compounds showed a variable but lower inhibitory effect. Compound **4e** was the most effective inhibitory compound in MCF-7 cells.

Immunofluorescence localization of tubulin in liver cancer cells

The localization of tubulin was explored in HepG2 cell line after treatment with selected promising compounds

Table 1. Collective calculated IC_{50} (μM) from linear equation of dose–response curve for compounds **4a**–**n** against hepatocarcinoma HepG2, breast adenocarcinoma MCF-7, colon carcinoma DLD-1, and leukemia HL-60 cells.

Compound no.	IC_{50}[a] (μM)			
	HepG2	MCF-7	DLD-1	HL-60
4a	30.97 ± 4.5	25.39 ± 2.31	26.22 ± 1.75	28.01 ± 3.5
4b	151.43 ± 4.62	164.83 ± 4.1	173.88 ± 3.32	132.52 ± 2.22
4c	31.07 ± 2.27	71.18 ± 3.5	38.32 ± 2.9	27.27 ± 1.9
4d	58.39 ± 2.65	50.28 ± 1.1	68.29 ± 2.11	53.22 ± 1.42
4e	15.43 ± 0.91	7.79 ± 0.82	27.59 ± 1.81	12.97 ± 0.88
4f	15.94 ± 1.12	10.79 ± 0.93	21.64 ± 1.12	11.49 ± 1.01
4g	33.50 ± 2.5	8.40 ± 1.11	39.67 ± 1.99	30.28 ± 1.65
4h	127.63 ± 1.87	26.66 ± 1.03	167.86 ± 2.91	102.97 ± 2.01
4i	163.12 ± 5.61	30.52 ± 2.32	176.72 ± 2.95	151.02 ± 4.01
4j	36.20 ± 1.8	45.32 ± 2.25	40.37 ± 3.01	34.02 ± 1.23
4k	46.77 ± .099	14.34 ± 0.45	54.29 ± 1.0	42.85 ± 1.25
4l	19.55 ± 1.02	13.20 ± 1.51	38.01 ± 1.19	13.13 ± 0.61
4m	70.89 ± 1.56	14.08 ± 0.09	79.80 ± 1.11	66.24 ± 1.78
4n	30.39 ± 0.98	28.62 ± 1.24	54.06 ± 1.56	27.80 ± 1.12

[a] IC_{50} = compound concentration required to inhibit tumor cell viability by 50%. Data are expressed as the mean ± SE from the dose–response curves of at least three experiments.

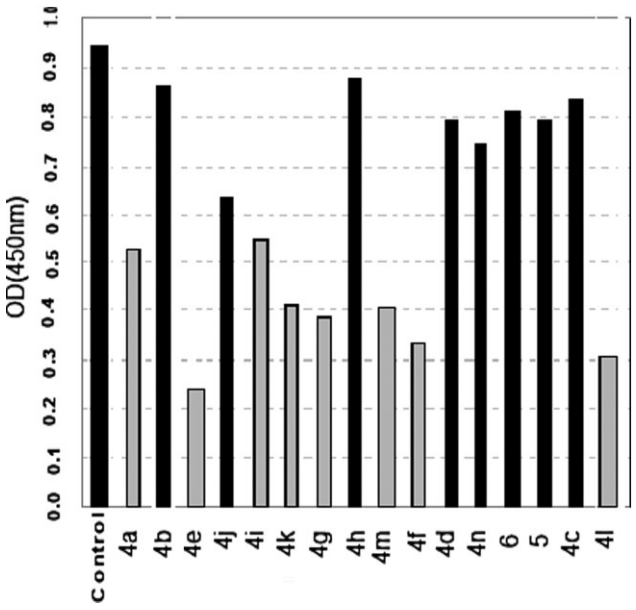

Figure 2. Level of tubulin in MCF-7 cells after treatment for 24 h by tested compounds. Black bars represent inactive compounds, and gray bars represent promising tubulin inhibiting compounds (around 50% inhibition).

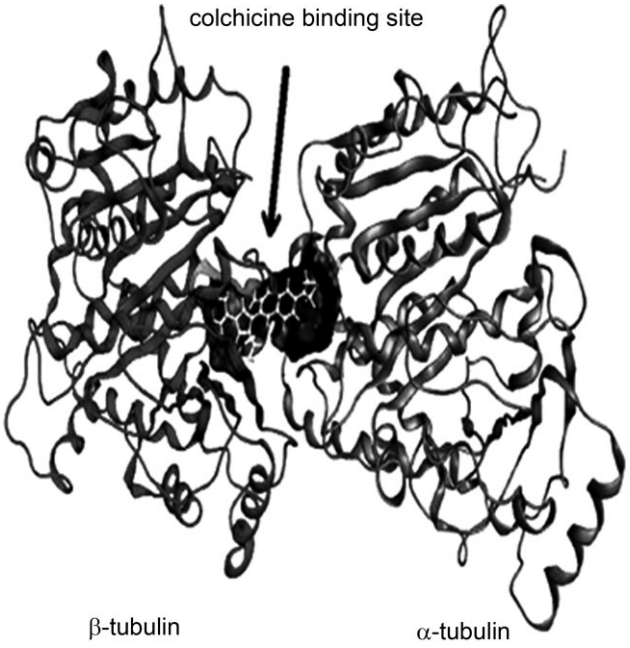

Figure 4. Colchicine binding site between α and β subunits of tubulin.

that revealed an inhibitory effect on tubulin as indicated by ELISA. Cells were treated with 25 μg/mL of each compound for 48 h, and then submitted to immunofluorescence labeling and analysis under fluorescence microscope. The treatment of hepatocellular carcinoma HepG2 cells revealed that compound **4f** showed a moderate inhibitory effect on cellular tubulin formation (Fig. 3), as concluded from the inhibition of the fluorescence intensity (about 65% of that of the original control tubulin).

Molecular docking study results with tubulin protein

Inspection of the colchicines binding site revealed that colchicine site is mostly buried in the intermediate domain of the β subunit. Colchicine also interacts with loop T5 of the neighboring α subunit (Fig. 4) [30].

All the tested compounds (**4e**, **4f**, and **4l**) showed similar binding to colchicines and inhibition of tubulin protein. The results of interaction energies with tubulin protein are shown in Table 2. Molecular docking simulation of compounds **4e** and **4f** into tubulin protein active site was done. They got

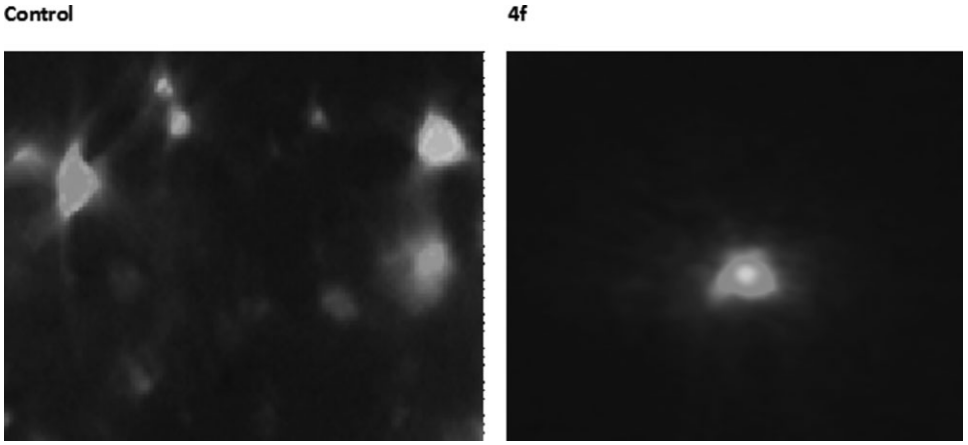

Figure 3. Fluorescence intensity (IFU) of tubulin localization in HepG2 cells after treatment with **4f** for 24 h compared to control cells.

Table 2. Interaction energies of compounds (**4d**, **4e**, **4f**, and **4l**) with tubulin protein.

Compound no.	Δ*G* (kcal/mol)
4d	−10.4857
4e	−15.3932
4f	−13.6294
4l	−10.4586

stabilized at the colchicine-binding site of tubulin by hydrophobic and hydrogen bond interactions (Fig. 5A and B).

The trimethoxyphenyl is oriented at hydrophobic pocket composed of Leu248β, Ala316β, Val318β, Met259β, Ile378β, and Ala354β. The 3 and 4 OCH_3-substitutions can form hydrogen bonds with Cys241 in β-subunit (3.82 or 4.98 Å).

In addition, several molecular interactions were considered to be responsible for the observed affinity. Two hydrogen bonds between carbonyl group of the ligand and Ala250β were found and the other between O in dimethoxyphenyl of the ligand and Ser178α. Also, there were van der Waals interactions between the benzene ring of the ligand and Lys254β, Asn249β, and Gln11α.

Compound **4l** showed different flipped binding mode than compounds **4e** and **4f** as the more lipophilic difluorophenyl ring being oriented in the hydrophobic pocket, as shown in Fig. 5C.

The *para* substituent is out the pocket of the DAMA–colchicine–tubulin complex as shown in Fig. 5D, which may explain the decreased cytotoxic and tubulin polymerization inhibitory activity in the *para* substituted anilides.

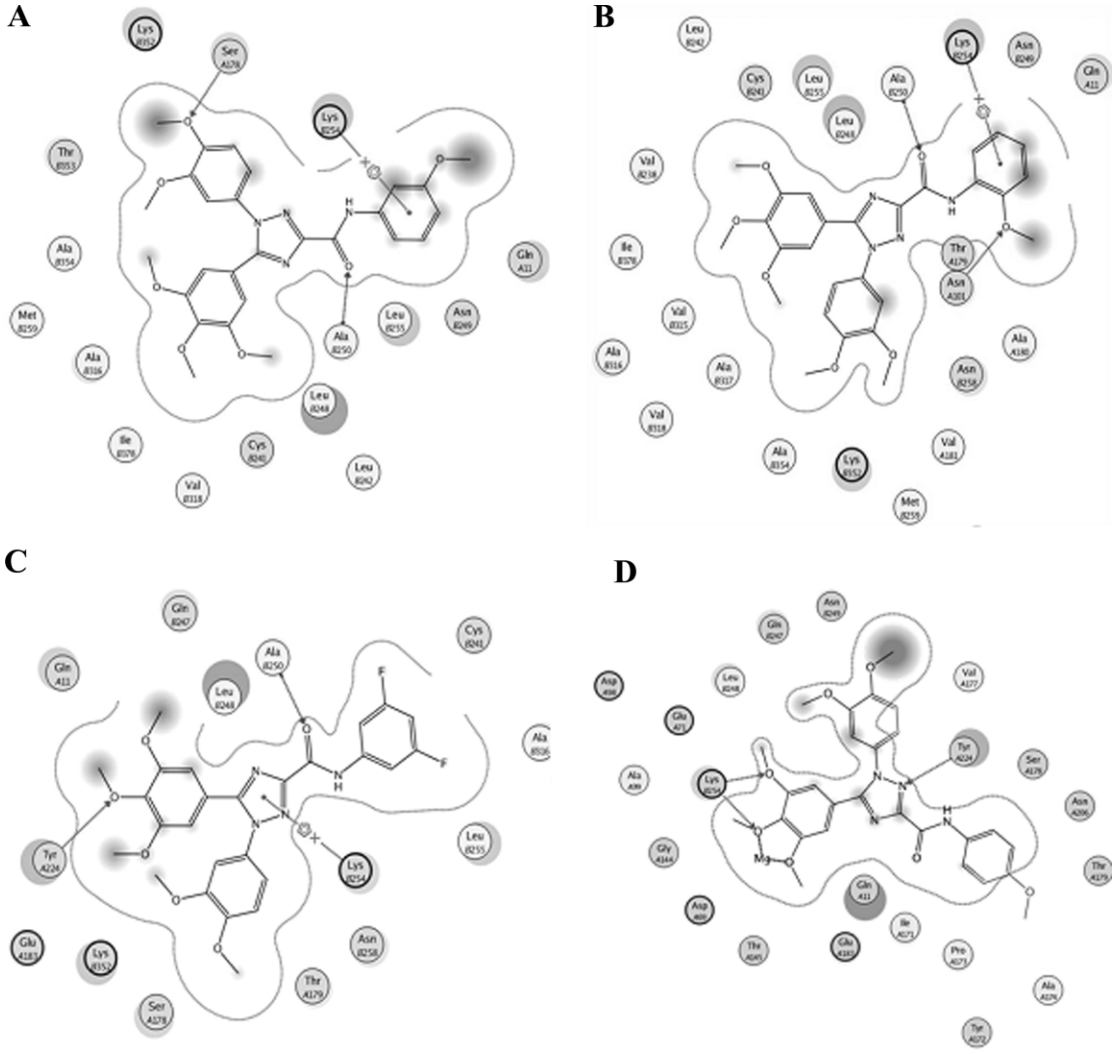

Figure 5. 2D representation of docking of compounds **4e** (A), **4f** (B), **4l** (C), and **4d** (D) into the colchicine binding site in the tubulin protein.

Conclusions

A group of novel 1-(4-methoxyphenyl)-5-(3,4,5-trimethoxyphenyl)-1*H*-1,2,4-triazole-3-carboxanilides was prepared and characterized by different spectroscopic and elemental analysis techniques. Only *ortho* and *meta* substituted anilides showed the highest activity while the *para* substitution showed a decrease in the activity. The compounds showed the highest degree of tubulin polymerization inhibition, only those compounds of highest cytotoxic activity. In conclusion, the prepared 1-(4-methoxyphenyl)-5-(3,4,5-trimethoxyphenyl)-1*H*-1,2,4-triazole-3-carboxylic acid derivatives are revealed as promising anticancer agents, stimulating the study of their full structure–activity relationship.

Experimental

Chemistry

Melting points were determined on Stuart electrothermal melting point apparatus and were uncorrected. IR spectra were recorded on Nicolet iS5 FT-IR spectrometer at Minia University. NMR spectra were carried out using a Bruker Avance 300 MHz NMR spectrometer, using TMS as internal reference. Chemical shifts (δ values are given in parts per million (ppm) relative to $CDCl_3$ (7.29 for proton and 76.9 for carbon) or DMSO-d_6 (2.50 for proton and 39.50 for carbon) and coupling constants (J) in Hertz. Splitting patterns are designated as follows: s, singlet; d, doublet; t, triplet; q, quartet; dd, doublet of doublet; m, multiplet. The progress of reactions and the purity of the prepared compounds were monitored by thin-layer chromatography (TLC) using Merck 9385 pre-coated aluminum plate silica gel (Kieselgel 60) 5 cm $\times$ 20 cm plates with a layer thickness of 0.2 mm. The spots were detected by exposure to UV-lamp at $\lambda = 254$ nm. Elemental analysis was performed on Vario El Elementar CHN Elemental analyzer; organic microanalysis section, Cairo University, Giza, Egypt and the results were within $\pm$0.4% of the theoretical values.

*Synthesis of 4-(2-(3,4-dimethoxyphenyl)hydrazono)-2-(3,4,5-trimethoxyphenyl)oxazol-5(4H)-one **3***

Trimethoxyhippuric acid **1** (0.26 mol, 70.00 g) in acetic anhydride (100 mL) was heated for 30 min or until a clear solution of **2** was obtained; this solution was cooled to room temperature (solution A). To a cold solution of 3,4-dimethoxyaniline (0.2 mol, 30.64 g) in 5 N HCl (60 mL) in an ice-salt bath -5 to 0°C, a solution of sodium nitrite (0.26 mol, 17.94 g) in water (30 mL) was added in a dropwise manner. The reaction mixture was left for 10 min (solution B). Solution A was added to solution B in presence of anhydrous sodium acetate (0.36 mol, 30 g). The reaction mixture was stirred at 0–10°C for 2 h; the formed precipitate was filtered off and dried (dark red solid, yield 70%).

*General procedure for the synthesis of 1-(3,4-dimethoxyphenyl)-5-(3,4,5-trimethoxyphenyl)-1H-1,2,4-triazole-3-carboxanilides (**4a–n**)*

A mixture of compound **3** (4.15 g, 0.01 mol) and appropriate primary aromatic amine (0.01 mol) was refluxed in acetic acid (50 mL) in the presence of anhydrous sodium acetate (1.5 g, 0.018 mol) for 2 h. The reaction mixture was cooled and poured into ice water (50 mL). The formed precipitate was filtered off, dried, and recrystallized from aqueous methanol.

*1-(3,4-Dimethoxyphenyl)-N-phenyl-5-(3,4,5-trimethoxyphenyl)-1H-1,2,4-triazole-3-carboxamide **4a***

Brown crystals (3.28 g, 67% yield); m.p. 90–92°C; IR (KBr) (cm^{-1}): 3315 (NH), 1691 (CO), 1595 (C=N); ^{1}H NMR (300 MHz, $CDCl_3$) δ (ppm): 3.69 (s, 6H, $2OCH_3$), 3.84 (s, 9H, $3OCH_3$), 6.84 (s, 2H, Ar–H), 7.12–7.17 (m, 3H, Ar–H), 7.37–7.56 (m, 4H, Ar–H), 7.86 (d, 2H, $J = 8.10$ Hz, Ar–H), 10.50 (s, 1H, NH); ^{13}C NMR (75 MHz, DMSO-d_6) δ (ppm): 57.73 and 62.07 (OCH_3), 107.76, 115.91, 121.83, 123.32, 125.29, 129.01, 129.73, 131.47, 139.16, 140.01,153.42, 155.33, 156.65, and 158.08 (aromatic carbons), 160.75 (C=O). Anal. calcd. for $C_{26}H_{26}N_4O_6$ (490.19): C, 63.66; H, 5.34; N, 11.42. Found: C, 63.38; H, 5.0; N, 11.56.

*1-(3,4-Dimethoxyphenyl)-N-(p-tolyl)-5-(3,4,5-trimethoxyphenyl)-1H-1,2,4-triazole-3-carboxamide **4b***

Pale brown crystals (2.77 g, 55% yield); m.p. 75–77°C; IR (KBr) (cm^{-1}): 3331 (NH), 1691 (CO), 1589 (C=N); ^{1}H NMR (300 MHz, $CDCl_3$) δ (ppm): 2.32 (s, 3H, CH_3), 3.69 (s, 6H, $2OCH_3$), 3.84 (s, 9H, $3OCH_3$), 6.78 (s, 2H, Ar–H), 6.89 (q, 2H, Ar–H), 7.01 (s, 1H, Ar–H), 7.16 (d, 2H, $J = 8.1$ Hz, Ar–H), 7.62 (d, 2H, $J = 8.4$ Hz, Ar–H), 8.96 (s, 1H, CONH). ^{13}C NMR (75 MHz, $CDCl_3$) δ (ppm): 20.84 ($ArCH_3$), 56.01, 56.14, 56.21, 60.86 (OCH_3), 106.25, 109.17, 110.75, 118.24, 121.75, 129.51, 130.65, 134.23, 134.79, 149.47, 149.85, 153.08, 154.71, and 156.08 (aromatic carbons), 156.59 (C=O). Anal. calcd. for $C_{27}H_{28}N_4O_6$ (504.53): C, 64.27; H, 5.59; N, 11.10. Found: C, 64.43; H, 5.57; N, 11.33.

*1-(3,4-Dimethoxyphenyl)-N-(o-tolyl)-5-(3,4,5-trimethoxyphenyl)-1H-1,2,4-triazole-3-carboxamide **4c***

Pale brown powder (2.87 g, 57% yield); m.p. 80–83°C; IR (KBr) (cm^{-1}): 3341 (NH), 1690 (CO), 1585 (C=N); ^{1}H NMR (300 MHz, $CDCl_3$) δ (ppm): 2.38 (s, 3H, CH_3), 3.69 (s, 6H, $2OCH_3$), 3.90 (s, 9H, $3OCH_3$), 6.80 (s, 2H, Ar–H), 6.87–6.95 (p, 2H, Ar–H), 7.10 (t, 2H, Ar–H), 7.24 (q, 2H, Ar–H), 8.10 (d, 1H, $J = 8.1$ Hz, Ar–H), 8.96 (s, 1H, CONH). ^{13}C NMR (75 MHz, $CDCl_3$) δ (ppm): 17.69 ($ArCH_3$), 56.03, 56.16, 56.23, and 60.89 (OCH_3), 106.32, 109.25, 110.79, 118.32, 121.83, 122.46, 125.23, 126.86, 130.43, 135.20, 149.47, 149.88, 153.08, 154.78, and 156.08 (aromatic carbons), 156.79 (C=O). Anal. calcd. for $C_{27}H_{28}N_4O_6$ (504.53): C, 64.27; H, 5.59; N, 11.10. Found: C, 64.5; H, 5.27; N, 11.41.

*1-(3,4-Dimethoxyphenyl)-N-(4-methoxyphenyl)-5-(3,4,5-trimethoxyphenyl)-1H-1,2,4-triazole-3-carboxamide **4d***

Yellowish brown powder (3.08 g, 59% yield); m.p. 184–185°C; IR (KBr) (cm^{-1}): 3340 (NH), 1691 (CO), 1592 (C=N); ^{1}H NMR (300 MHz, $CDCl_3$) δ (ppm): 3.69 (s, 6H, $2OCH_3$), 3.84 (s, 12H, $4OCH_3$), 6.78 (s, 2H, Ar–H), 6.86 (d, 2H, $J = 9$ Hz, Ar–H), 6.89 (d, 1H, $J = 2.1$ Hz, Ar–H), 6.92 (d, 1H, $J = 3.9$ Hz, Ar–H), 7.02 (d, 1H, $J = 1.8$ Hz, Ar–H), 7.65 (d, 2H, $J = 9$ Hz, Ar–H), 8.91 (s, 1H, CONH). ^{13}C NMR (75 MHz, $CDCl_3$) δ (ppm): 55.42, 56.03, 56.16, 56.23, and 60.87 (OCH_3), 106.25, 109.19, 110.75, 114.18, 118.25, 121.47, 121.81, 130.53, 130.70, 149.47, 149.85, 153.10, 154.70, 156.15, and 156.51 (aromatic carbons), 156.54 (C=O). Anal. calcd. for $C_{27}H_{28}N_4O_7$ (520.53): C, 62.30; H, 5.42; N, 10.76. Found: C, 62.79; H, 4.93; N, 10.90.

1-(3,4-Dimethoxyphenyl)-N-(3-methoxyphenyl)-5-(3,4,5-trimethoxyphenyl)-1H-1,2,4-triazole-3-carboxamide ***4e***

Yellowish powder (3.07 g, 59% yield); m.p. 78–81°C; IR (KBr) (cm^{-1}): 3351 (NH), 1691 (CO), 1589 (C=N); ^{1}H NMR (300 MHz, $CDCl_3$) δ (ppm): 3.72 (s, 6H, $2OCH_3$), 3.84 (s, 3H, OCH_3), 3.87 (s, 3H, OCH_3), 3.88 (s, 3H, OCH_3), 3.93 (s, 3H, OCH_3), 6.72 (d, 1H, $J = 7.2$ Hz, Ar–H), 6.81 (s, 2H, Ar–H), 6.90 (d, 1H, $J = 8.4$ Hz, Ar–H), 6.93 (d, 1H, $J = 2.1$ Hz, Ar–H), 7.05 (s, 1H, Ar–H), 7.27 (d, 2H, $J = 9$ Hz, Ar–H), 7.53 (s, 1H, Ar–H), 9.02 (s, 1H, CONH). ^{13}C NMR (75 MHz, $CDCl_3$) δ (ppm): 55.25, 56.05, 56.16, 56.23, and 60.87 (OCH_3), 105.56, 106.29, 109.17, 110.79, 118.24, 121.75, 130.65, 138.53, 149.49, 149.88, and 153.10, 155.98, and 156.71 (aromatic carbons), 160.14 (C=O). Anal. calcd. for $C_{27}H_{28}N_4O_7$ (520.53): C, 62.30; H, 5.42; N, 10.76. Found: C, 62.55; H, 5.19; N, 11.11.

1-(3,4-Dimethoxyphenyl)-N-(2-methoxyphenyl)-5-(3,4,5-trimethoxyphenyl)-1H-1,2,4-triazole-3-carboxamide ***4f***

Reddish brown powder (3.22 g, 62% yield); m.p. 170–172°C; ^{1}H NMR (300 MHz, $CDCl_3$) δ (ppm): 3.68 (s, 6H, $2OCH_3$), 3.84 (s, 6H, $2OCH_3$), 3.90 (s, 6H, $2OCH_3$), 6.80 (s, 2H, Ar–H), 6.85–7.10 (m, 6H, Ar–H), 8.57 (dd, 1H, $J = 1.5$ and 1.5 Hz, Ar–H), 9.57 (s, 1H, CONH). ^{13}C NMR (75 MHz, $CDCl_3$) δ (ppm): 55.70, 55.98, 56.11, 56.18, and 60.83 (OCH_3), 106.34, 109.27, 109.91, 110.74, 118.32, 120.10, 121.02, 121.91, 148.22, 149.41, 149.79, 153.00, 154.71, and 156.35 (aromatic carbons), 156.63 (C=O). Anal. calcd. for $C_{27}H_{28}N_4O_7$ (520.53): C, 62.30; H, 5.42; N, 10.76. Found: C, 62.64; H, 5.16; N, 11.0.

N,1-bis(3,4-Dimethoxyphenyl)-5-(3,4,5-trimethoxyphenyl)-1H-1,2,4-triazole-3-carboxamide ***4g***

Dark red powder (3.40 g, 62% yield); m.p. 83–85°C; IR (KBr) (cm^{-1}): 3339 (NH), 1690 (CO), 1589 (C=N); ^{1}H NMR (300 MHz, $CDCl_3$) δ (ppm): 3.71 (s, 6H, $2OCH_3$), 3.87 (s, 9H, $3OCH_3$), 3.93 (s, 6H, $2OCH_3$), 6.80 (s, 2H, Ar–H), 6.857–6.921 (m, 3H, Ar–H), 7.03 (s, 1H, Ar–H), 7.16 (d, 1H, $J = 8.4$ Hz, Ar–H), 7.58 (s, 1H, Ar–H), 8.91 (s, 1H, CONH). ^{13}C NMR (75 MHz, $CDCl_3$) δ (ppm): 55.98, 56.13, 56.24, 56.29, 60.78, and 60.97 (OCH_3), 104.79, 106.35, 106.86, 109.20, 110.85, 111.40, 118.27, 121.88, 130.76, 131.06, 146.13, 153.10, and 153.21 (aromatic carbons), 156.64 (C=O). Anal. calcd. for $C_{28}H_{30}N_4O_8$ (550.56): C, 61.08; H, 5.49; N, 10.18. Found: C, 61.08; H, 5.27; N, 10.32.

N-(4-Bromophenyl)-1-(3,4-dimethoxyphenyl)-5-(3,4,5-trimethoxyphenyl)-1H-1,2,4-triazole-3-carboxamide ***4h***

Light blue powder (3.29 g, 58% yield); m.p. 170–172°C; IR (KBr) (cm^{-1}): 3345 (NH), 1695 (C=O), 1589 (C=N); ^{1}H NMR (300 MHz, $CDCl_3$) δ (ppm): 3.67 (s, 6H, $2OCH_3$), 3.83 (s, 6H, $2OCH_3$), 3.89 (s, 3H, OCH_3), 6.76 (s, 2H, Ar–H), 6.85 (d, 2H, $J = 8.7$ Hz, Ar–H), 6.99 (s, 1H, Ar–H), 7.44 (d, 2H, $J = 8.7$ Hz, Ar–H), 7.64 (d, 2H, $J = 8.7$ Hz, Ar–H), 9.01 (s, 1H, CONH). ^{13}C NMR (75 MHz, $CDCl_3$) δ (ppm): 56.00, 56.13, 56.19, and 60.84 (OCH_3), 106.25, 109.12, 110.74, 117.10, 118.22, 121.30, 136.42, 139.90, 149.46, 149.88, 153.07, 154.81, and 155.72 (aromatic carbons), 156.68 (C=O). Anal. calcd. for $C_{26}H_{25}BrN_4O_6$ (569.40): C, 54.84; H, 4.43; N, 9.84. Found: C, 54.54; H, 4.07; N, 10.02.

1-(3,4-Dimethoxyphenyl)-N-(4-fluorophenyl)-5-(3,4,5-trimethoxyphenyl)-1H-1,2,4-triazole-3-carboxamide ***4i***

Yellowish brown powder (3.01 g, 59% yield); m.p. 78–80°C; IR (KBr) (cm^{-1}): 3350 (NH), 1691 (CO), 1589 (C=N); ^{1}H NMR (300 MHz, $CDCl_3$) δ (ppm): 3.67 (s, 6H, $2OCH_3$), 3.83 (s, 6H, $2OCH_3$), 3.89 (s, 3H, OCH_3), 6.76 (s, 2H, Ar–H), 6.87 (s, 2H, Ar–H), 7.03 (t, 3H, $J = 8.7$ Hz Ar–H), 7.69 (s, 2H, Ar–H), 9.01 (s, 1H, CONH). ^{13}C NMR (75 MHz, $CDCl_3$) δ (ppm): 55.98, 56.11, 56.18, 60.83, 106.22, 109.12, 110.75, 115.50, 115.80, 118.20, 121.48, 133.35, 139.88, 149.46, 149.88, 153.07, 154.78, 155.80, and 161.03 (aromatic carbons), 156.68 (C=O). Anal. calcd. for $C_{26}H_{25}FN_4O_6$ (508.18): C, 61.90; H, 4.80; N, 11.11. Found: C, 61.51; H, 4.84; N, 11.27.

N-(2,3-Difluorophenyl)-1-(3,4-dimethoxyphenyl)-5-(3,4,5-trimethoxyphenyl)-1H-1,2,4-triazole-3-carboxamide ***4j***

Dark brown powder (2.98 g, 57% yield); m.p. 74–76°C; IR (KBr) (cm^{-1}): 3351 (NH), 1691 (CO), 1589 (C=N); ^{1}H NMR (300 MHz, $CDCl_3$) δ (ppm): 3.70 (s, 6H, $2OCH_3$), 3.86 (s, 9H, $3OCH_3$), 6.79 (s, 2H, Ar–H), 6.86–6.98 (m, 4H, Ar–H), 7.01–7.12 (m, 1H, Ar–H), 8.30 (t, 1H, Ar–H), 9.26 (s, 1H, CONH). ^{13}C NMR (75 MHz, $CDCl_3$) δ (ppm): 56.05, 56.18, 56.24, and 60.89 (OCH_3), 106.32, 109.22, 110.84, 112.17, 116.74, 118.34, 121.58, 130.63, 149.54, 150.00, 153.12, 155.01, and 155.54 (aromatic carbons), 156.81 (C=O). Anal. calcd. for $C_{26}H_{24}F_2N_4O_6$ (526.49): C, 59.31; H, 4.59; N, 10.64. Found: C, 59.36; H, 4.29; N, 10.80.

N-(3,4-Difluorophenyl)-1-(3,4-dimethoxyphenyl)-5-(3,4,5-trimethoxyphenyl)-1H-1,2,4-triazole-3-carboxamide ***4k***

Brown powder (2.79 g, 53% yield); m.p. 73–75°C; IR (KBr) (cm^{-1}): 3339 (NH), 1694 (CO), 1589 (C=N); ^{1}H NMR (300 MHz, $CDCl_3$) δ (ppm): 3.69 (s, 6H, $2OCH_3$), 3.85 (s, 6H, $2OCH_3$), 3.91 (s, 3H, OCH_3), 6.77 (s, 2H, Ar–H), 6.89 (s, 2H, Ar–H), 7.00 (s, 1H, Ar–H), 7.13 (d, 1H, $J = 9.3$ Hz, Ar–H), 7.31 (s, 1H, Ar–H), 7.84 (s, 1H, Ar–H) 9.01 (s, 1H, CONH). ^{13}C NMR (75 MHz, $CDCl_3$) δ (ppm): 56.05, 56.18, 56.24, and 60.91 (OCH_3), 106.27, 109.14, 110.80, 115.50, 117.17, 118.25, 121.57, 149.56, 150.00, 153.15, 154.93, and 155.59 (aromatic carbons), 156.76 (C=O). Anal. calcd. for $C_{26}H_{24}F_2N_4O_6$ (526.49): C, 59.31; H, 4.59; N, 10.64. Found: C, 59.09; H, 4.39; N, 10.43.

N-(3,5-Difluorophenyl)-1-(3,4-dimethoxyphenyl)-5-(3,4,5-trimethoxyphenyl)-1H-1,2,4-triazole-3-carboxamide ***4l***

Yellowish brown powder (3.09 g, 59% yield); m.p. 70–72°C; IR (KBr) (cm^{-1}): 3332 (NH), 1690 (CO), 1589 (C=N); ^{1}H NMR (300 MHz, $CDCl_3$) δ (ppm): 3.67 (s, 6H, $2OCH_3$), 3.84 (s, 6H, $2OCH_3$), 3.90 (s, 3H, OCH_3), 6.58 (s, 1H, Ar–H), 6.75 (s, 2H, Ar–H), 6.88 (s, 2H, Ar–H), 6.99 (s, 1H,Ar–H), 7.36 (d, 2H, $J = 6.9$ Hz, Ar–H), 9.13 (s, 1H, CONH). ^{13}C NMR (75 MHz, $CDCl_3$) δ (ppm): 56.01, 56.14, 56.21, 60.87, and (OCH_3), 102.74, 103.12, 106.27, 109.11, 110.79, 118.24, 121.43, 139.40, 149.52, 150.00, 153.12, 154.99, and 155.37 (aromatic carbons), 156.84 (C=O). Anal. calcd. for $C_{26}H_{24}F_2N_4O_6$ (526.49): C, 59.31; H, 4.59; N, 10.64. Found: C, 59.44; H, 4.54; N, 10.60.

1-(3,4-Dimethoxyphenyl)-N-(2,3,4-trifluorophenyl)-5-(3,4,5-trimethoxyphenyl)-1H-1,2,4-triazole-3-carboxamide ***4m***

Yellowish brown powder (3.12 g, 57% yield); m.p. 70°C; ^{1}H NMR (300 MHz, $CDCl_3$) δ (ppm): 3.67 (s, 6H, $2OCH_3$), 3.84 (s, 6H, $2OCH_3$), 3.88 (s, 9H, $3OCH_3$), 6.77 (s, 2H, Ar–H), 6.81–7.04 (m, 4H, Ar–H), 8.17–8.25 (m, 1H, Ar–H), 9.12 (s, 1H, CONH). ^{13}C NMR (75 MHz, $CDCl_3$) δ (ppm): 55.98, 56.14, 56.19, and 60.84 (OCH_3), 106.25 (CH), 109.15 (CH), 110.79 (CH), 111.66 (CH), 115.75 (CH), 118.29 (CH), 121.47 (CH), 139.98, 149.51, 149.98, 153.07, 154.99, and 155.31 (aromatic carbons), 156.87 (CO). Anal. calcd. for $C_{26}H_{23}F_3N_4O_6$ (544.48): C, 57.35; H, 4.26; N, 10.29. Found: C, 57.19; H, 3.98; N, 10.51.

1-(3,4-Dimethoxyphenyl)-N-(naphthalen-1-yl)-5-(3,4,5-trimethoxyphenyl)-1H-1,2,4-triazole-3-carboxamide **4n**

Reddish brown powder (3.79 g, 70% yield); m.p. 88–90°C; IR (KBr) (cm^{-1}): 3336 (NH), 1696 (CO), 1589 (C=N); ^{1}H NMR (300 MHz, $CDCl_3$) δ (ppm): 3.71 (s, 6H, $2OCH_3$), 3.88 (s, 6H, $2OCH_3$), 3.92 (s, 3H, OCH_3), 6.84 (s, 2H, Ar–H), 6.92 (m, 2H, Ar–H), 7.06 (s, 1H, Ar–H), 7.53 (m, 3H, Ar–H), 7.73 (d, 1H, $J = 8.4$ Hz, Ar–H), 7.89 (d, 1H, $J = 9$ Hz, Ar–H), 8.04 (d, 1H, $J = 7.5$ Hz, Ar–H), 8.28 (d, 1H, $J = 7.2$ Hz, Ar–H), 9.56 (s, 1H, CONH). ^{13}C NMR (75 MHz, $CDCl_3$) δ (ppm): 56.09, 56.19, 56.28, and 60.92 (OCH_3), 106.39, 109.30, 110.84, 118.37, 120.03, 120.49, 121.85, 125.72, 125.92, 126.00, 126.28, 128.79, 130.76, 131.72, 134.06, 149.54, 149.95, 153.15, 153.93, and 156.26 (aromatic carbons), 157.29 (C=O). Anal. calcd. for $C_{30}H_{28}N_4O_6$ (540.56): C, 66.66; H, 5.22; N, 10.36. Found: C, 66.51; H, 5.0; N, 10.34.

Biology

Cell culture

Human hepatocarcinoma cell line (HepG2), breast adenocarcinoma cell line (MCF-7), colon carcinoma (DLD-1), and leukemia (HL-60), which were purchased from ATCC, USA, were used to evaluate the cytotoxic effect of the tested samples. Cells were routinely cultured in Dulbecco's modified Eagle's medium (DMEM). Media was supplemented with 10% fetal bovine serum (FBS), 2 mM L-glutamine, containing 100 units/mL of penicillin G sodium, 100 units/mL of streptomycin sulfate, and 250 ng/mL amphotericin B. Cells were maintained at sub-confluence at 37°C in humidified air containing 5% CO_2. For sub-culturing, monolayer cells were harvested after trypsin/EDTA treatment at 37°C. Cells were used when confluence had reached 75%. Tested samples were dissolved in dimethyl sulfoxide (DMSO), and then diluted thousand times in the assay to begin with the indicated concentration. All cell culture material was obtained from Cambrex BioScience (Copenhagen, Denmark). All chemicals were from Sigma/Aldrich (USA), except mentioned. All experiments were repeated three times, unless mentioned.

Anti-tumor activity

Cytotoxicity of tested samples was measured against each cell line using the MTT cell viability assay. MTT (3-[4,5–dimethylthiazole-2-yl]-2,5-diphenyltetrazolium bromide) assay is based on the ability of active mitochondrial dehydrogenase enzyme of living cells to cleave the tetrazolium rings of the yellow MTT and form a dark blue, insoluble formazan crystal, which is largely impermeable to cell membranes, resulting in its accumulation within healthy cells. Solubilization of the cells results in the liberation of crystals, which are then solubilized. The number of viable cells is directly proportional to the level of soluble formazan dark blue color. The extent of the reduction of MTT was quantified by measuring the absorbance at 570 nm [31]. Briefly, cells (0.5×10^5 cells/well), in serum-free media, were plated in a flat bottom 96-well microplate, and treated with 20 μL of serial concentrations of the tested samples for 48 h at 37°C, in a humidified 5% CO_2 atmosphere. After incubation, media were removed and 40 μL of MTT solution (5 mg/mL of MTT in 0.9% NaCl) in each well was added and incubated for an additional 4 h. MTT crystals were solubilized by adding 180 μL of acidified isopropanol/well and the plate was shaken at room temperature, followed by photometric determination of the absorbance at 570 nm using microplate ELISA reader. Triplicate repeats were performed for each concentration and the average was calculated. Data were expressed as the percentage of relative viability compared with the untreated cells compared with the vehicle control, with cytotoxicity indicated by <100% relative viability. Percentage of relative viability was calculated using the following equation: [absorbance of treated cells/absorbance of control cells)] × 100. Then the half maximal inhibitory concentration (IC_{50}) was calculated from the equation of the dose–response curve (linear regression).

$$Y = a^*X + b$$

$$IC_{50} = \frac{(0.5 - b)}{a}$$

where drug concentrations x_1, x_2, ..., x_n and growth inhibition y_1, y_2, ..., y_n.

Cell lysate preparation

Cell lysate was prepared to be used in ELISA. The treated and untreated cells were trypsinized, washed, and centrifuged for 10 min at 1000*g*. Cell pellet was lysed in 0.5 mL of ice-cold lysis buffer [50 mM Tris–HCl, 150 mM NaCl, 1 mM EGTA, 1 mM EDTA, 20 mM NaF, 100 mM Na_3VO_4, 0.5% NP40, 1% Triton X-100, 1 mM phenylmethylsulfonyl fluoride, 10 mg/mL aprotinin, and 10 mg/mL leupeptin (pH 7.4)]. Cell lysates were passed through a 21-gauge needle to break up cell aggregates, and then centrifuged at 14,000*g* for 15 min at 4°C. The supernatants (total cell lysate) were submitted to ELISA and lipid peroxides estimation. The total protein content of the lysates was measured according to Smith et al. [32], by bicinchoninic acid (BCA) and using bovine serum albumin (BSA) as a standard (data not mentioned).

Evaluation of tubulin

Tubulin level was estimated in cell lysates by indirect ELISA. All steps of indirect ELISA were followed according to the method modified by Gamal-Eldeen et al. [33], with some modifications, in which 96-well flat bottom polystyrene plates were coated with cell lysates samples (100 μL/well). After overnight incubation at 4°C, the plates were washed and then 200 μL of blocking buffer was delivered into each well. The plates were covered and incubated for 1.5 h at 37°C and after a washing step, rabbit polyclonal antibody to tubulin (Abcam, Inc., Cambridge, MA, USA) was adjusted to 0.2 μg/mL and dispensed as (100 μL/well); after 1 h incubation at 37°C the plates were washed and the 100 μL/well of polyclonal goat anti-rabbit peroxidase-conjugate diluted 1:1000 was added and the plates were incubated for another 1 h at 37°C. At the end of the incubation period, the plates were washed, and the substrate solution was prepared (equal volumes of 3′,5,5′-tetramethyl benzidine (TMB) and H_2O_2; Kirkegaard and Perry Labs, Gaithersburg, MD). Color development was stopped by the addition of 100 μL/well of stopping buffer (1 M HCl). The color intensity was measured at 450 nm using the microplate reader (FLUOstar OPTIMA; BMG Labtech GmbH, Offenburg, Germany). The levels of tubulin in the cell lysate were expressed as milliabsorbance.

Immunofluorohistochemical evaluation of tubulin

Immunohistochemical detection of tubulin in fixed cells was followed according to the method originally developed by Kawahira [34], with some modifications.

Reagents preparation: 0.1 M Citrate buffer pH to 6.0: 9 mL of 0.1 M citric acid solution was added to 41 mL of 1 M sodium citrate solution and the volume was adjusted to 500 mL by deionized water.

Antigen retrieval solution: 50 mL of 0.1 M citrate buffer, 500 μL of Triton-100, and 250 μL of Tween-20 were mixed together and the final volume was adjusted to 500 mL by deionized water.

Blocking solution: 50 mL of 0.1 M citrate buffer, 500 μL of Triton 100, 250 μL of Tween-20, and 25 mL of FBS were mixed together and the final volume was adjusted to 500 mL by deionized water.

Procedure: Slides of fixed cells were rinsed in three changes of PBS. Antigen retrieval step, by which the availability of the antigen for interaction with a specific antibody is maximized, was performed by immersing slides in antigen retrieval solution and incubated in a water bath at 95–99°C for 20 min. Afterwards, slides were directly transferred to pre-cooled antigen retrieval solution placed at −4°C for 5 min. Non-specific binding of the antibody is prevented by incubating the slides in blocking solution at 37°C for 30 min. Slides were then incubated for 30 min at 37°C with rabbit anti-human tubulin antibody (1:500) diluted with blocking solution. Excess antiserum was rinsed from the slide by immersing in cold buffer for two changes of 5–10 min each. Slides were then incubated at 37°C with goat FITC-anti rabbit IgG (1:2500) diluted with blocking solution. The slides were rinsed in the enzyme substrate till the color developed. Images were visualized using a fluorescence microscope (Axiostar Plus, Zeiss, Goettingen, Germany) equipped with image analyzer and digital camera (PowerShot A20, Canon, USA).

Docking studies

Docking simulation study was performed using Molecular Operating Environment (MOE), 2010.10; Chemical Computing Group, Inc. (Montreal, QC, Canada, 2013). The computational software operated under "Windows XP" installed on an Intel Pentium IV PC with a 1.6 GHz processor and 512 MB memory.

Target compounds optimization

The target compounds were constructed into a 3D model using the builder interface of the MOE program. After checking their structures and the formal charges on atoms by 2D depiction, the following steps were carried out: the target compounds were subjected to a conformational search. All conformers were subjected to energy minimization; all the minimizations were performed with MOE until a RMSD gradient of 0.01 kcal/mol and RMS distance of 0.1 Å with MMFF94X force-field and the partial charges were automatically calculated. The obtained database was then saved as MDB file to be used in the docking calculations.

Optimization of the enzymes active site

The X-ray crystallographic structure of tubulin complexed with colchicine was obtained from the Protein Data Bank through the Internet (http://www. rcsb.org/, PDB code 1SA0) [30]. The enzyme was prepared for docking studies: hydrogen atoms were added to the system with their standard geometry. The atoms connection and type were checked for any errors with automatic correction. Selection of the receptor and its atoms potential were fixed. MOE Alpha Site Finder was used for the active site search in the enzyme structure using all default items. Dummy atoms were created from the obtained alpha spheres.

Docking of the target molecules to tubulin protein in colchicine binding site

Docking of the conformation database of the target compounds was done using MOE-Dock software. The following methodology was generally applied: the enzyme active site file was loaded and the Dock tool was initiated. The program specifications were adjusted to: Dummy atoms as the docking site, triangle matcher as the placement methodology to be used. London dG as scoring methodology to be used was adjusted to its default values. The MDB file of the ligand to be docked was loaded and Dock calculations were run automatically. The obtained poses were studied and the poses showing best ligand–enzyme interactions were selected and stored for energy calculations.

The authors acknowledge the Science and Technology Development Fund (STDF) Egypt (Project No. 2943 Basic and Applied Research) for funding this work.

The authors have declared no conflict of interest.

References

[1] E. Hamel, *Med. Res. Rev.* **1996**, *16*, 207–231.

[2] J. Fahy, B. T. Hill, *Curr. Pharm. Des.* **2001**, *7*, 1297–1301.

[3] N. H. Nam, *Curr. Med. Chem.* **2003**, *10*, 1697–1722.

[4] H. P. Hsieh, J. P. Liou, N. Mahindroo, *Curr. Pharm. Des.* **2005**, *11*, 1655–1677.

[5] G. M. Tozer, V. E. Prise, J. Wilson, R. J. Locke, B. Vojnovic, M. R. Stratford, M. F. Dennis, D. J. Chaplin, *Cancer Res.* **1999**, *59*, 1626–1634.

[6] G. M. Tozer, C. Kanthou, C. S. Parkins, S. A. Hill, *Int. J. Exp. Pathol.* **2002**, *83*, 21–38.

[7] G. G. Dark, S. A. Hill, V. E. Prise, G. M. Tozer, G. R. Pettit, D. J. Chaplin, *Cancer Res.* **1997**, *57*, 1829–1834.

[8] K. Grosios, S. E. Holwell, A. T. McGown, G. R. Pettit, M. C. Bibby, *Br. J. Cancer* **1999**, *81*, 1318–1327.

[9] A. Dowlati, K. Robertson, M. Cooney, W. P. Petros, M. Stratford, J. Jesberger, N. Rafie, B. Overmoyer, V. Makkar, B. Stambler, A. Taylor, J. Waas, J. S. Lewin, K. R. McCrae, S. C. Remick, *Cancer Res.* **2002**, *62*, 3408–3416.

[10] J. P. Stevenson, M. Rosen, W. Sun, M. Gallagher, D. G. Haller, D. Vaughn, B. Giantonio, R. Zimmer, W. P. Petros, M. Stratford, D. Chaplin, S. L. Young, M. Schnall, P. J. O'Dwyer, *J. Clin. Oncol.* **2003**, *21*, 4428–4438.

[11] I. G. Kirwan, P. M. Loadman, D. J. Swaine, D. A. Anthoney, G. R. Pettit, J. W. Lippert, S. D. Shnyder, P. A. Cooper, M. C. Bibby, *Clin. Cancer Res.* **2004**, *10*, 1446–1453.

[12] S. M. Galbraith, R. J. Maxwell, M. A. Lodge, G. M. Tozer, J. Wilson, N. J. Taylor, J. J. Stirling, L. Sena, A. R. Padhani, G. J. Rustin, *J. Clin. Oncol.* **2003**, *21*, 2831–2842.

[13] R. LeBlanc, J. Dickson, T. Brown, M. Stewart, H. N. Pati, D. VanDerveer, H. Arman, J. Harris, W. Pennington, H. L. Holt, M. Lee, *Bioorg. Med. Chem.* **2005**, *13*, 6025–6034.

[14] C. M. Lin, S. B. Singh, P. S. Chu, R. O. Dempcy, J. M. Schmidt, G. R. Pettit, E. Hamel, *Mol. Pharmacol.* **1988**, *34*, 200–208.

[15] K. Ohsumi, T. Hatanaka, K. Fujita, R. Nakagawa, Y. Fukuda, Y. Nihei, Y. Suga, Y. Morinaga, Y. Akiyama, T. Tsuji, *Bioorg. Med. Chem. Lett.* **1998**, *8*, 3153–3158.

[16] L. Wang, K. W. Woods, Q. Li, K. J. Barr, R. W. McCroskey, S. M. Hannick, L. Gherke, R. B. Credo, Y. H. Hui, K. Marsh, R. Warner, J. Y. Lee, N. Zielinski-Mozng, D. Frost, S. H. Rosenberg, H. L. Sham, *J. Med. Chem.* **2002**, *45*, 1697–1711.

[17] G. R. Pettit, M. R. Rhodes, D. L. Herald, E. Hamel, J. M. Schmidt, R. K. Pettit, *J. Med. Chem.* **2005**, *48*, 4087–4099.

[18] G. R. Pettit, M. P. Grealish, D. L. Herald, M. R. Boyd, E. Hamel, R. K. Pettit, *J. Med. Chem.* **2000**, *43*, 2731–2737.

[19] M. Medarde, A. C. Ramos, E. Caballero, R. Pelaez-Lamamie de Clairac, J. L. Lopez, D. G. Gravalos, A. S. Feliciano, *Bioorg. Med. Chem. Lett.* **1999**, *9*, 2303–2308.

[20] N. H. Nam, Y. Kim, Y. J. You, D. H. Hong, H. M. Kim, B. Z. Ahn, *Bioorg. Med. Chem. Lett.* **2001**, *11*, 3073–3076.

[21] N. H. Nam, Y. Kim, Y. J. You, D. H. Hong, H. M. Kim, B. Z. Ahn, *Bioorg. Med. Chem. Lett.* **2002**, *12*, 1955–1958.

[22] C. C. Kuo, H. P. Hsieh, W. Y. Pan, C. P. Chen, J. P. Liou, S. J. Lee, Y. L. Chang, L. T. Chen, C. T. Chen, J. Y. Chang, *Cancer Res. 64*, **2004**, 4621–4628.

[23] C. Borrel, S. Thoret, X. Cachet, D. Guenard, F. Tillequin, M. Koch, S. Michel, *Bioorg. Med. Chem. 13*, **2005**, 3853–3864.

[24] X. Ouyang, E. L. Piatnitski, V. Pattaropong, X. Chen, H. Y. He, A. S. Kiselyov, A. Velankar, J. Kawakami, M. Labelle, L. Smith, J. Lohman, S. P. Lee, A. Malikzay, J. Fleming, J. Gerlak, Y. Wang, R. L. Rosler, K. Zhou, S. Mitelman, M. Camara, D. Surguladze, J. F. Doody, M. C. Tuma, *Bioorg. Med. Chem. Lett. 16*, **2006**, 1191–1196.

[25] K. Metwally, O. Aly, E. Aly, A. Banerjee, R. Ravindra, S. Bane, *Bioorg. Med. Chem.* **2007**, *15*, 2434–2440.

[26] M. Abdel-Aziz, O. M. Aly, S. Khan, K. Mukherjee, S. Bane, *Arch. Pharm. Chem. Life Sci.* **2012**, *345*, 535–548.

[27] G. W. Sawdey, *J. Am. Chem. Soc.* **1957**, *79*, 1955–1956.

[28] S. M. Rabea, N. A. El-Koussi, H. Y. Hassan, T. Aboul-Fadl, *Arch. Pharm. Chem. Life Sci.* **2006**, *339*, 32–40.

[29] Y. Q. Liu, X. J. Li, C. Y. Zhao, X. Nan, J. Tian, S. L. Morris-Natschke, Z. J. Zhang, X. M. Yang, L. Yang, L. H. Li, X. W. Zhou, K. H. Lee, *Bioorg. Med. Chem.* **2013**, *21*, 1248–1256.

[30] R. B. G. Ravelli, B. Gigant, P. A. Curmi, I. Jourdain, S. Lachkar, A. Sobel, M. Knossow, *Nature* **2004**, *428*, 198–202.

[31] M. B. Hansen, S. E. Nielsen, K. Berg, *J. Immunol. Methods* **1989**, *119*, 203–210.

[32] P. K. Smith, R. I. Krohn, G. T. Hermanson, A. K. Mallia, F. H. Gartner, M. D. Provenzano, E. K. Fujimoto, N. M. Goeke, B. J. Olson, D. C. Klenk, *Anal. Biochem.* **1985**, *150*, 76–85.

[33] A. M. Gamal-Eldeen, S. M. El-Daly, I. H. Borai, H. A. Wafay, A.-R. B. Abdel-Ghaffar, *Photodiagn. Photodyn. Ther.* **2013**, *10*, 446–459.

[34] K. Kawahira, *Arch. Dermatol. Forsch.* **1999**, *291*, 413–418.

